

Quantization in Multispectral Color Image Acquisition

*Peter D. Burns and Roy S. Berns**

Eastman Kodak Company, Rochester, New York, USA

**Munsell Color Science Laboratory,*

Chester F. Carlson Center for Imaging Science

Rochester Institute of Technology, Rochester, New York, USA

Abstract

For applications where colorimetric information is insufficient to characterize an input scene or document, multispectral image capture (*i.e.* for more than three records) has been suggested.^{1,3} Experimental cameras have been described, as have the results of signal processing to extract useful spectral and colorimetric information. Previous reports have addressed both system accuracy and precision, the latter as influenced by random pixel-to-pixel image noise. Another contributor to system precision is signal quantization. Statistics are computed for various levels of uniform and non-uniform quantization. The resulting errors in the estimated object spectral reflectance factor and subsequent colorimetric transformation are addressed. The comparison of these errors with those due to stochastic noise sources indicates that both are influenced by the image processing employed.

Introduction

The color accuracy of multispectral image-acquisition systems is usually evaluated in terms of color-errors due to spectral sensitivities, the number of records, or the approximation inherent in linear models of object characteristics. The precision of such systems is influenced not only by stochastic error sources such as detector shot-noise,⁴ but also the signal encoding and arithmetic precision used for signal processing. In this presentation we analyze the effect of camera signal quantization for a previously described approach to multispectral image capture.⁵

Image quantization is the encoding of each sample of a continuous signal, *e.g.* radiance, as one of a limited number of discrete values. When image signals are quantized prior to other signal processing, the resultant error can be propagated through the signal path in a similar way to that used for stochastic error propagation.⁶ However in this case, the errors form a finite set, are discrete, and represent a bias in the original and transformed signal.

Camera System

The multispectral camera was formed by acquiring several frames using a set spectral filters and monochrome digital camera. The set of seven commercially available

filters was chosen to sample the visible wavelength range at intervals of approximately 50 nm. The digital camera analyzed in conjunction with the filter set yields the combined spectral response given in Fig. 1. This corresponds to the set of interference filters used with the Kodak DCS 100 electronic camera.

As previously reported,⁵ principal component analysis can be used to reconstruct spectral reflectance curves from camera signals. A least-square matrix, \mathbf{M} , was calculated to allow the seven camera signals, $\{s\}$, to be transformed to estimates of the scalar coefficients associated with the eigenvectors, $\{e\}$, to reconstruct the spectra. The spectral reconstruction, expressed in matrix notation, is given by,

$$\mathbf{f} = \Phi \mathbf{M} \mathbf{s} \quad (1)$$

where \mathbf{f} is the reconstructed spectral reflectance vector, $\mathbf{s} = [s_1, s_2, \dots, s_7]^T$, $\Phi = [e_1, e_2, \dots, e_5]^T$.

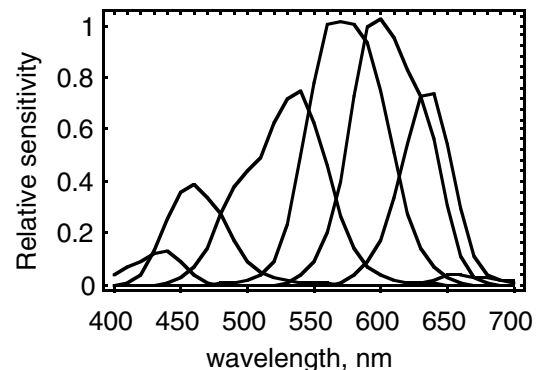


Figure 1. The spectral sensitivity of each of the seven filter/sensor channels (left-right:1-7).

For specified viewing conditions the CIE tristimulus values, $\mathbf{t} = [X, Y, Z]^T$, for each pixel can be computed using an ASTM weight vector.⁷ This is given by, $\mathbf{t} = \mathbf{W} \mathbf{f}$, where \mathbf{W} is the weight vector. Combining this operation with that of Eq. (1), the tristimulus vector, \mathbf{t} , can be computed from the seven camera signals

$$\mathbf{t} = \mathbf{W} \Phi \mathbf{M} \mathbf{s}. \quad (2)$$

Quantization

For an m -record image acquisition, we take the set of quantization intervals for a given signal location (in m -space) as that spanned by incrementing and decrementing each of the m signals by one interval, and comparing it with the reference location. This results in $3^m - 1$ intervals. For a given system the effective quantization intervals can be computed by processing them as ordinary pixel values through the signal processing path.

Consider a simple three-record colorimeter which detects sample tristimulus values, X, Y, Z . For a given signal quantization scheme and reference color, the set of $3^3 = 27$ signal values is

$$\mathbf{s} = \{(X_{ref}, Y_{ref}, Z_{ref}), (X_{ref} + \Delta_X, Y_{ref}, Z_{ref}), (X_{ref} - \Delta_X, Y_{ref}, Z_{ref}), (X_{ref} + \Delta_X, Y_{ref} + \Delta_Y, Z_{ref}), \dots, (X_{ref} + \Delta_X, Y_{ref} + \Delta_Y, Z_{ref} + \Delta_Z)\},$$

where $(X_{ref}, Y_{ref}, Z_{ref})$ are the reference signal values and $(\Delta_X, \Delta_Y, \Delta_Z)$ are the quantization intervals for each signal. Each of the above set of signals can be transformed into a secondary color-space and the set of 26 differences (from the reference signal) computed.

The influence of camera signal quantization on system performance for a multispectral camera can be addressed in the same way. Now, however, the set of quantization intervals about a given color is much larger. For the seven-filter camera, $3^7 - 1 = 2186$ intervals need to be investigated. This was done in a computed experiment as outlined in Fig. 2. Note that the second step is used to introduce nonlinear quantization intervals. The camera signals for each of the twenty-four ColorChecker samples were calculated assuming the copy stand source, and the camera-filter sensitivities of Fig. 1. These signals were then quantized, either uniformly ($p = 1$) or as a power function ($p = 0.33, 0.42$). The remaining signal path included a modified PCA spectral reconstruction and transformation to CIELAB, for illuminant D_{65} and the 10° observer. Computed average color-differences due to signal quantization are given in Table I, for several schemes. By introducing the nonlinear quantization ($p \neq 1$), the average and median ΔE_{ab}^* were reduced by about 0.11. This had less effect when ten- or twelve-bit encoding was used. As might be expected, increasing the bits/signal used (thereby increasing the number of levels by a factor 2 per bit) reduced the CIELAB quantization intervals by about the same factor.

The CIELAB coordinates corresponding to the set of quantized camera signals for the Cyan sample of the Gretag Macbeth ColorChecker chart is shown in Figure 3. This example used an eight-bit uniform quantizer. For this multivariate discrete distribution, we can compute the covariance matrix

$$\Sigma_{L^*a^*b^*} = \begin{bmatrix} 0.042 & -0.101 & 0.085 \\ -0.101 & 0.934 & -0.322 \\ 0.085 & -0.322 & 0.288 \end{bmatrix}. \quad (3a)$$

Taking the square-root of the diagonal elements of the above matrix yields the root-mean-square quantization interval from the mean value,

$$rms_q(L^*, a^*, b^*) = [0.21, 0.93, 0.53]. \quad (3b)$$

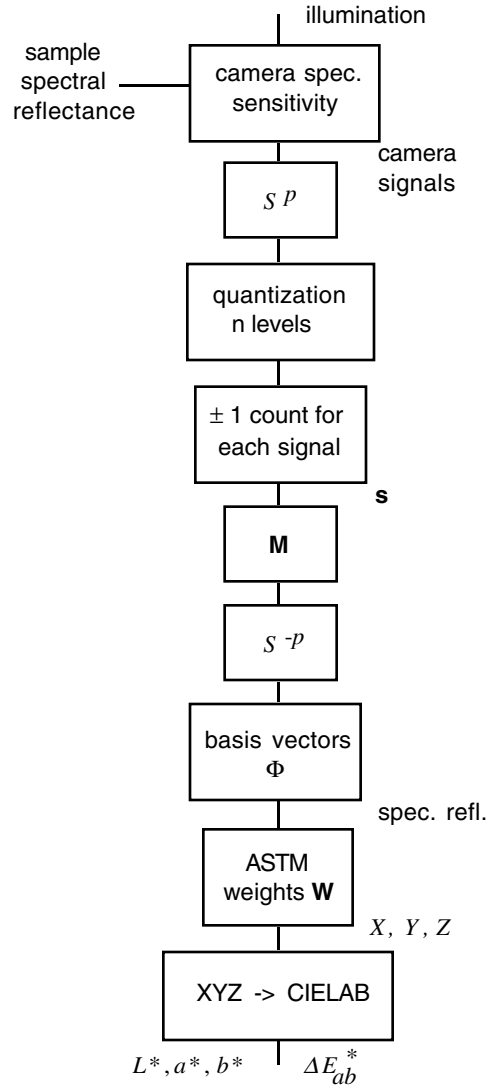


Figure 2. Analysis of signal quantization for the multispectral camera and spectral reconstruction via modified PCA method.

This is consistent with the plot in Fig. 3, which shows the largest range along the a^* axis. So although the set of quantized signal values, \mathbf{s} , formed a discrete uniform distribution in 7-space, the signal processing modified the relative magnitude of the errors. This is to be expected, since the matrices of Eq.(2) introduce covariance into the quantization distribution in the same way that they do for stochastic image noise sources.^{4,6}

Table I: Quantization interval as average ΔE_{ab}^* color difference values, for several levels of signal encoding and camera signal selections. Calculation was based on simulation of multispectral capture of the 24 ColorChecker sample colors, and modified PCA reconstruction.

signals	Bits	Exp.p	mean	median	max
7 (1-7)	8	1	1.08	1.03	2.38
	8	0.42	1.04	0.97	2.83
	8	0.33	0.95	0.91	2.12
	10	1	0.27	0.26	0.59
	10	0.42	0.26	0.24	0.70
	10	0.33	0.28	0.23	0.53
	12	1	0.07	0.07	0.14
	12	0.42	0.07	0.06	0.18
	12	0.33	0.07	0.07	0.19
5 (12357)	10	1	0.29	0.29	0.54
	10	0.42	0.23	0.22	0.44
	10	0.33	0.25	0.24	0.47
	12	1	0.07	0.07	0.14
	12	0.42	0.06	0.05	0.11
	12	0.33	0.06	0.06	0.12

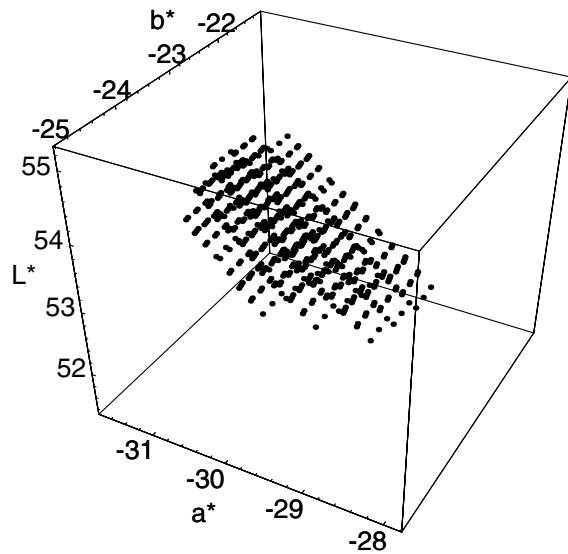


Figure 3. Distribution of CIELAB coordinates for the set of quantized camera signals and eight-bit uniform encoding, for the Cyan sample.

Comparison with Stochastic Image Noise

A key aspect of signal encoding is the identification of the important information in the signal(s) to be processed. For a given system, it is natural to compare error introduced by primary (camera) signal quantizing to that due to other sources. As previously described,⁵ the image noise

introduced in image detection and storage can be estimated by analyzing the pixel statistics for nominally uniform areas, such as those in the ColorChecker test chart. This was done for a range of color samples. The RMS noise characteristics for each of the seven camera (filter + detector) channels were similar, shown in Fig. 4.

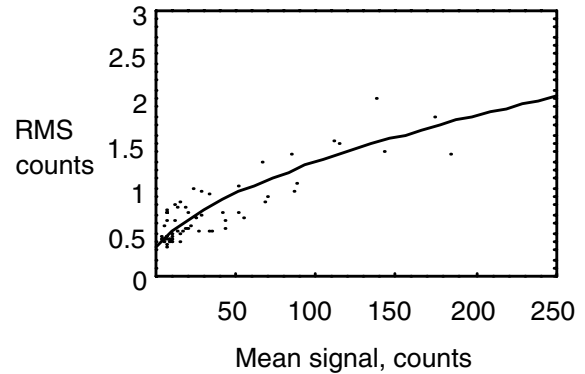


Figure 4. Camera RMS noise levels at the detector expressed as 8-bit digital code values (counts).

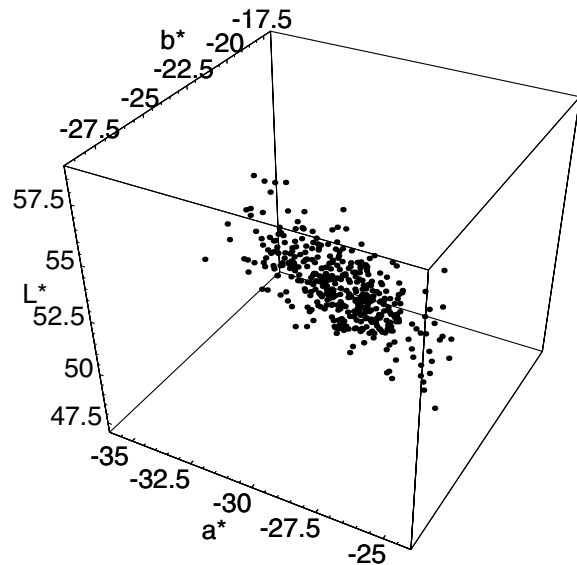


Figure 5. Distribution of CIELAB coordinates for the Cyan color sample, based on camera data for 400 pixels. Note that axes are longer than in Fig. 3.

A uniform image area of 400 pixels for the Cyan color sample was processed such that a spectral reconstruction via Eq.(1) was computed for each pixel. From these data the corresponding CIELAB coordinates were computed in similar fashion to the set of quantized signals, s . The results are plotted in Figure 5, with axes 50% longer than in Fig. 3. The corresponding covariance matrix and RMS values are,

$$\Sigma_{L^*a^*b^*} = \begin{bmatrix} 0.167 & -0.465 & 0.262 \\ -0.465 & 4.583 & -1.752 \\ 0.262 & -1.752 & 1.709 \end{bmatrix} \quad (4a)$$

$$rms_n(L^*, a^*, b^*) = [0.41, 2.14, 1.31]. \quad (4b)$$

Comparing the Eqs. (3) with (4) shows the similarity in the form of the covariance matrix (*i.e.* underlying correlation) introduced in signal processing. In addition for this Cyan color sample, the errors introduced by quantization are substantially less than those due to stochastic sources. Note however, that the pixel data of Fig. 4 and Eqs. (4) include 8-bit encoded error.

Conclusions

The evaluation of image signal quantization error in the context of multispectral image capture and signal processing has been addressed. Errors introduced due to primary signal encoding can be analyzed as a set of (color) differences by incrementing and decrementing each signal level and processing the resulting values. Quantization can also be compared with sources of random error. This was demonstrated, and both sources were seen to be influenced by the image processing path.

References

1. M. L. Simpson and J. F. Jansen, *Appl. Opt.*, **30**: 4666 (1991).
2. K. Martinez, J. Cupitt and D. Saunders, High Resolution Colorimetric Imaging of Paintings, *Proc. SPIE*, **1901**, pg. 25. (1993).
3. T. Keusen and W. Praefcke, Multispectral Color System with an Encoding Format Compatible to Conventional Tristimulus Model, *Proc. IS&T/SID Third Color Imaging Conf.*, pg. 112. (1995).
4. P. D. Burns and R. S. Berns, Image Noise and Colorimetric Precision in Multispectral Image Capture, *Proc. IS&T/SID Sixth Color Imaging Conf.*, pg. 83, (1998).
5. P. D. Burns and R. S. Berns, Analysis of Multispectral Image Capture, *Proc. IS&T/SID Fourth Color Imaging Conf.*, IS&T/SID, pg. 19, (1996).
6. P. D. Burns and R. S. Berns, *Color Research and Application*, **22**: 280, (1997).
7. *Standard Test Method for Computing the Colors of Objects by Using the CIE System, E308 - 90*, American National Standards Institute, NY, 1990.